Clogging of an Alpine streambed by silt-sized particles – Insights from laboratory and field experiments

Journal Article

Author(s):
Fetzer, Jasmin; Holzner, Markus; Plötze, Michael; Furrer, Gerhard

Publication date:
2017-12-01

Permanent link:
https://doi.org/10.3929/ethz-b-000192701

Originally published in:
Water Research 126, https://doi.org/10.1016/j.watres.2017.09.015

Water Research 126 (2017) 60–69

Contents lists available at ScienceDirect

Water Research

journal homepage: www.elsevier.com/locate/watres

Clogging of an Alpine streambed by silt-sized particles – Insights from laboratory and field experiments

Jasmin Fetzer [a, *], Markus Holzner [b], Michael Plötze [c], Gerhard Furrer [a]

[a] ETH Zurich, Institute of Biogeochemistry and Pollutant Dynamics, 8092 Zürich, Switzerland
[b] ETH Zurich, Institute of Environmental Engineering, 8093 Zürich, Switzerland
[c] ETH Zurich, Institute for Geotechnical Engineering, 8093 Zürich, Switzerland

ARTICLE INFO

Article history:
Received 27 March 2017
Received in revised form
24 August 2017
Accepted 4 September 2017
Available online 7 September 2017

Keywords:
Clogging
Hyporheic zone
Column experiment
Silt-sized suspended particles
Field experiment

ABSTRACT

Clogging of streambeds by suspended particles (SP) can cause environmental problems, as it can negatively influence, e.g., habitats for macrozoobenthos, fish reproduction and groundwater recharge. This especially applies in the case of silt-sized SP. Until now, most research has dealt with coarse SP and was carried out in laboratory systems. The aims of this study are to examine (1) whether physical clogging by silt-sized SP exhibits the same dynamics and patterns as by sand-sized SP, and (2) the comparability of results between laboratory and field experiments.

We carried out vertical column experiments with sand-sized bed material and silt-sized SP, which are rich in mica minerals. In laboratory experiments, we investigated the degree of clogging quantified by the reduction of porosity and hydraulic conductivity and the maximum clogging depth as a function of size and shape of bed material, size of SP, pore water flow velocity, and concentration of calcium cations. The SP were collected from an Alpine sedimentation basin, where our field experiments were carried out. To investigate the clogging process in the field, we buried columns filled with sand-sized quartz in the stream bed.

We found that the maximal bed-to-grain ratio where clogging still occurs is larger for silt-sized SP than for sand-sized SP. The observed clogging depths and the reduction of flow rate through the column from our laboratory experiments were comparable to those from the field. However, our field results showed that the extent of clogging strongly depends on the naturally-occurring hydrological dynamics. The field location was characterized by a more polydisperse suspension, a strongly fluctuating water regime, and high SP concentrations at times, leading to more heterogeneous and more pronounced clogging when compared to laboratory results.

1. Introduction

In streambeds several ecological functions might be affected by clogging as they are the main habitats for invertebrates and several fish species (Einstein, 1968; Schälchli, 1992). In general, alteration of sediment regimes can influence the physical characteristics of a streambed, and the anthropogenically caused input of fine sediments into riverine systems has evolved into a major environmental issue (Datry et al., 2015). One important effect is clogging, that is infiltration and accumulation of inorganic and organic material in the streambed. This can lead to the reduction of permeability and porosity (Grischek and Bartak, 2016) and may cause consolidation of streambeds and a reduced exchange between surface water and groundwater. As a consequence, oxygen and nutrients may be limited in the hyporheic zone, and the groundwater recharge can be reduced, affecting stream biodiversity and biogeochemistry (Datry et al., 2015; Schälchli, 1992; Wooster et al., 2008).

In this work, the effect of mainly physical and, to a limited extent, chemical parameters on clogging were examined. We note, however, that in nature, biological and chemical parameters may significantly affect the clogging process, for example due to the presence of algae or biofilms. Physical clogging might also be a precondition for biological clogging processes (Nogaro et al., 2010;

* Corresponding author. ETH Zurich, CHN F50.2, Universitaetstrasse 8, CH-8092, Zurich, Switzerland.

E-mail addresses: jasmin.fetzer@wsl.ch (J. Fetzer), holzner@ifu.baug.ethz.ch (M. Holzner), michael.ploetze@igt.baug.ethz.ch (M. Plötze), gerhard.furrer@env.ethz.ch (G. Furrer).

http://dx.doi.org/10.1016/j.watres.2017.09.015

Rink-Pfeiffer et al., 2000). Physical clogging of pores occurs when suspended particles (SP) are transported along the flow path and then are retained, leaving pores located below the clogged ones devoid of SP (Sakthivadivel and Einstein, 1970). This process has been actively researched since the pioneering work by Einstein (Einstein, 1968; Sakthivadivel and Einstein, 1970). Parameters that influence the clogging process are size, shape, and concentration of the SP, size and shape of the bed material, grain size distributions of SP and bed material, as well as the pore water flow velocity. Under field conditions, several afore mentioned parameters depend on the stream flow volume and velocity that affect the SP size distribution, the pore flow velocity, and the armour layer. The armour layer is a typical configuration found in stream beds. It is the natural uppermost bed layer consisting of material coarser than the layers below the armour layer and protects subjacent material from being washed off (Vericat et al., 2006).

Sources for fine SP can be found in natural and anthropogenically influenced environments. Certain geological formations such as mud stones can be a source for silt-sized SP. Anthropogenic sources for silt-sized SP include, for instance, human-induced erosions and landslides, land use (change), accidental releases from reservoirs, and hydroelectric plants (Benamar et al., 2007; Cui and Wilcox, 2008; Wooster et al., 2008). It is likely that the fraction of fine SP in rivers will increase due to anthropogenic activities, e.g. as shown by Bogen and Bonsnes (2001) when they noticed an increase in the clay-sized fraction of SP in surface waters after the implementation of a hydropower plant in Norway.

Until now, most research on physical clogging dealt with SP in the range of 80–500 μm on gravel substrate (Adams and Beschta, 1980; Beschta and Jackson, 1979; Diplas, 1994; Diplas and Parker, 1992; Einstein, 1968; Frostick et al., 1984; Gibson et al., 2010, 2009; Jackson, 1981; Sakthivadivel and Einstein, 1970; Schälchli, 1992; Siriwardene et al., 2007; Wooster et al., 2008). Few experiments with silt-sized SP (2–63 μm) were carried out (Alem et al., 2015; Bai et al., 2016; Benamar et al., 2007; Fries and Trowbridge, 2003). However, silt-sized SP play an important role in the clogging process, since they significantly decrease the porosity and have a large transport potential (Bai et al., 2016; McDowell-Boyer et al., 1986; Siriwardene et al., 2007). In contrast, sand-sized SP influence the porosity of the streambed only marginally as shown by field and laboratory experiments (Schälchli, 2002). It is not clear if the insights on clogging by sand-sized can be extrapolated to silt-sized SP, e.g. concerning the influence of particle size on the clogging depth (Huston and Fox, 2014). Furthermore, most recent studies were conducted in the laboratory without field application (Huston and Fox, 2014). Investigating the explicit role of SP in the silt-sized fraction on the clogging process in the laboratory and the field could further improve the clogging prediction.

By examining the clogging process on a small scale, the sealing of pores by SP can be explained by multi-particle bridging (Sakthivadivel and Einstein, 1970). SP are transported with the percolating water and eventually retained in pores. The maximum depth where particles are retained depends on parameters such as the bed-to-grain ratio (d_M/d_{SP}) and the pore water flow velocity. The bed-to-grain ratio is defined as the quotient of the bed material's diameter over the SP's diameter, defined as equivalent spherical diameter. Higher pore flow velocities favour the transport of larger particles, since it takes longer until they are retained in pores. This leads to a deeper intrusion of SP into the bed material (Alem et al., 2015; Benamar et al., 2007). Sealing occurs if several SP close a pore throat. The maximum depth, where multi-particle-bridges are found, is called the clogging depth Z_C. As particles accumulate in the bed, its hydraulic conductivity decreases. Attractive forces eventually counteract the drag caused by flow and gravitational forces, and the rate of transported particles decreases. Upwards from Z_C, pores are filled up to the armour layer until, finally, the pore water flow rate reaches a steady state. At this point, SP are no longer transported deeper into the bed, so long as conditions do not vary. The captured material exhibits an exponential profile with the highest amount of captured SP beneath the armour layer (Huston and Fox, 2014; and Fig. 1).

Two main parameters that were previously investigated were the bed-to-grain ratio and its relation to Z_C, as well as the thickness of the sealing layer that can be estimated from the bed grain diameter (Fig. 1). The assessment of the degree of clogging received renewed attention recently. In contrast to previous studies, Huston and Fox (2014) used the bed-to-grain ratio only for prediction whether or not clogging takes place. They further presented an improved formula for the critical bed-to-grain ratio for the initiation of clogging which included the gradation of the bed material (standard deviation $\sigma = SQRT(d_M^{85}/d_M^{15})$ as $d_M/(d_{SP}{}^*\sigma)$). To predict Z_C they suggested focusing on bed porosity and presented recently a momentum-impulse model to predict Z_C of fine sand in gravel beds (Fox, 2016; Huston and Fox, 2016). It is, however, not clear whether the model works for sand beds as well.

Overall, a high degree of clogging implies a strong reduction of porosity and hydraulic conductivity that can be caused by a deep clogging depth, a strong sealing layer, or a combination of both. The degree of clogging can be measured e.g. in the laboratory by the reduction of pressure and flow rate. However, it is more difficult to determine the degree of clogging in the field. Various clogging classification systems in the field have been discussed and proposed (Schälchli, 2002). Datry et al. (2015) and Grischek and Bartak (2016) proposed using hydraulic conductivity as an easily-measured clogging indicator in the field. This has the advantage of involving interstitial clogging, compared to previous approaches that focussed mainly on surface processes.

The main aims of this study are to determine (1) whether clogging with silt-sized SP exhibits the same dynamics and patterns

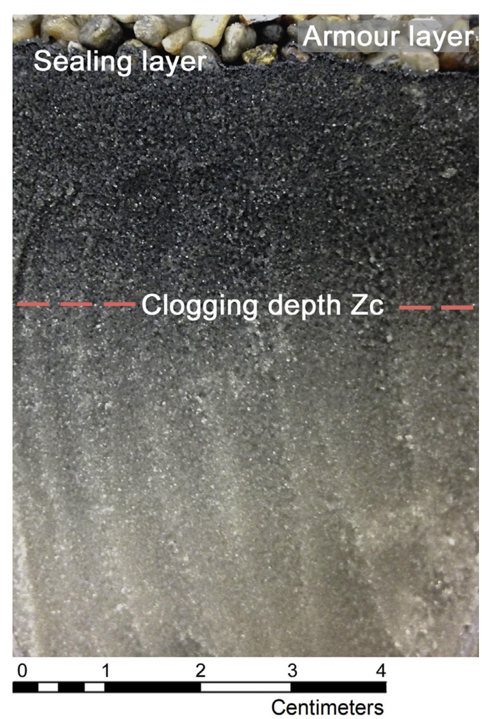

Fig. 1. Illustration of clogging depth, sealing and armour layer. Photographs from laboratory experiments with a profile with a decreasing number of retained particles with depth and a specific clogging depth Z_C.

as with coarser SP, and (2) if laboratory and field results are comparable and if the prioritization of influencing parameters on the degree of clogging differs between field and laboratory. Based on previous studies, we hypothesized:

The maximum bed-to-grain ratio where clogging occurs increases with the fineness of SP. Due to higher specific surface area, small SP may be more strongly attracted by bed material than coarse SP.

Higher Ca^{2+} concentrations (in the order of mM) cause smaller clogging depths than at lower concentrations. Divalent cations promote aggregation of SP and interaction with bed particles. Thus, clogging might be more pronounced.

Field experiments generally exhibit a higher degree of clogging than laboratory experiments. This may be explained by the high variation of stream water flow and the broad grain size span of transported SP.

To validate these hypotheses we conducted laboratory and field column experiments with fine SP (2–63 μm) and a sand-sized bed material.

2. Materials and methods

2.1. Laboratory investigations

We used vertical column experiments to investigate SP infiltration into a sand-sized bed material. Fig. 2 shows the experimental setup consisting of a suspension reservoir of 50 L that was stirred by nine fleas on a nine-position magnetic stirrer. The suspension was transported via a peristaltic pump (Ismatec, Switzerland) on top of the water-saturated column. The Plexiglas column had an inner diameter of 10 cm and a height of 40 cm. At the bottom, a 100 μm sieve kept the fine quartz particles in place. To obtain a homogenous bed, the column was packed by slowly pouring sand into deionized and degassed water. The water was filled from a Marriott's bottle into the column through the bottom so that the water level in the column was kept a few centimetres above the sand layer. The Marriott's bottle was used for filling of the column and detached during the experiments. The column was filled to approximately 20 cm. An armour layer with approximately 1 cm-sized gravel stones was added to keep the quartz sand in place

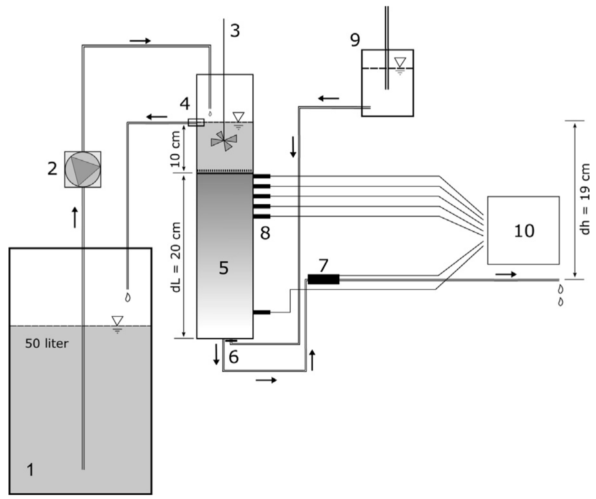

Fig. 2. Laboratory experimental design. (1) a 50 L reservoir for the suspension on a magnetic stirrer with 9 fleas; (2) peristaltic pump; (3) mechanical stirrer; (4) overflow pipe; (5) Plexiglas column filled with bed material and a gravel armour layer; (6) three-way valve; (7) flow meter; (8) pressure sensors (Keller); (9) Marriott's bottle with degassed and deionized water; (10) laptop. Not depicted is the camera that was used for monitoring of the clogging process.

and mimic an armour layer. The water level above the bed was kept at a constant level during the experiment (constant head). An overflow pipe at a height of 30 cm allowed the surplus water to flow back into the reservoir. Sedimentation in the column was avoided by using a mechanical stirrer to keep the supernatant suspension in motion. This fluid motion did not lead to dislocation of the sand grains which were protected by the armour layer. The bottom outlet was connected to a flow meter (SLQ-QT500 Liquid flow meter from Sensirion, Switzerland). Along the column, six pressure sensors (PAA-36XW from Keller Druckmesstechnik, Switzerland) were mounted. The first five sensors were spaced 1 cm apart, and the sixth was a further 11 cm distant. Specifications are presented in SI Table 1.

As bed material, we used two qualities of sand (ESEM images, SI Fig. 1a and b), rounded quartz sand (Carlo Bernasconi AG, Switzerland) and angular quartz sand (Gebrüder Dorfner, Germany, d_{50} value = 210 μm). The rounded quartz material was dry sieved to obtain a more mono-disperse fraction. This resulted in a d_{50} value of 400 μm (measured with a LA-950 Laser Particle Size Analyzer from Horiba Scientific).

Deposited material from our field study site (description in Section 2.2) in the Alpine sedimentation basin was used as SP (ESEM images, SI Fig. 1c and d). The parent material of the SP is a black, so-called paper shale, located in the upstream area of the study site. It exhibits a thin, laminated structure, and is darkly coloured. In general, black shales originate from organic carbon-rich sediments and the organic matter, being adsorbed to mineral surfaces, evokes the black colour (Kennedy et al., 2002; Tourtelot, 1979). For our samples, pycnometer (AccuPyc II 1340 V1.05) measurements revealed a grain density of 2.76 g/cm^3 for the grain size range of 5–20 μm. The samples consisted of approximately 40 wt% quartz, 30 wt% calcite, 10 wt% muscovite, and 10 wt% chlorite. The residual 10 wt% includes dolomite, pyrite, rutile, illite, and albite (measurements with an X-ray diffractometer D8 Advance, Bruker AXS, Germany). The mineral composition varied with particle size. The smaller the particles, the higher the mica mineral content, i.e., for particles <2 μm, muscovite accounted for more than 40 wt% and illite for more than 20 wt%, while quartz and calcite each contributed less than 5 wt% (König, 2014). In the stream water at the study site, the high content of these SP caused a spectacular phenomenon of shiny flow patterns that arises presumably because particles aligned with the flow's shear and make turbulent vortices visible. The flaky shape and a certain concentration of the particles might be crucial for appearance of the shiny flow patterns. With respect to the investigation of clogging one should keep in mind that particle orientation of certain minerals can also influence clogging mechanisms and the resultant clogging profile.

Two samples of bulk material were collected in the field from two spots with fine and well-fractionated sediments. They were used without sieving. The SP material sampled in August 2014 exhibited a size range of 14–16 μm, while the samples from October 2015 and August 2016 were finer (8–10 μm). The suspensions were prepared from the wet field samples since drying and re-suspending would affect the size and shape of the fragile aggregates. The material was suspended in deionized water at concentrations ranging between 1 and 4 g/L. Pre-experiments showed that concentrations within this range did not influence the clogging process.

The experiments were photographically monitored to document the process of clogging layer formation. The experiment was terminated when all 50 L of suspension had passed through the column, or when the flow rate reduced to a tenth of its initial value, whichever occurred first.

In addition to the entire series of laboratory experiments prepared with deionized water, one experiment with additional

0.8 mM $CaCl_2$ in the supernatant of the column was carried out. This corresponds to approximately half of Ca^{2+} concentrations found in the surface water at our field site. Pre-experiments revealed that this is approximately the critical aggregation concentration for promotion of particle aggregation, and higher concentrations do not further enhance aggregation and sedimentation. The pH measurements of the column's outflow showed no significant change resulting from $CaCl_2$ addition.

In total, six main laboratory experiments were carried out while varying the parameters (1) bed material size and shape, (2) SP size, (3) initial flow rate, and (4) concentration of Ca^{2+}. The experiments were designed in pairs, where a single parameter was varied between each pair.

2.2. Field investigations

The study site is located northeast of Piz Tasna, a mountain in the Swiss Alps (Fig. 3). It is a sedimentation basin with an area of approximately 2000 m^2 located at 2700 m a.s.l. and surrounded by moraines. The Aua da Tiral stream originates from the Vadret da Tasna glacier and surrounding snow cover, and is characterized by dense loads of silt-sized SP. It flows through the sedimentation basin, which is framed by coarse moraines. The sedimentation basin is clogged, and infiltration rates are hence very slow. The basin is structured by branching streams exhibiting seasonal and diurnal variations in course and water volume. Based on tracer field measurements during the experimental duration, flow velocity and discharge were estimated to range from 0.2 to 0.5 m/s and 30–200 L/s, respectively. Gravimetric particle concentration was measured at numerous times at three dates with time spans of 8 and 19 days in between. They ranged from 0.5 to 4.0 g/L. This variation was clearly visible. Thus, from our visual observations we can assume that this range was typical during almost three months of our field work. Within the sedimentation basin, the depth of the various stream branches ranged from very few to 40 cm. The sediment material is fractionated, from coarser material near the inlet of the basin to finer material towards the outlet. Several depth profiles from the basin showed that fine SP are found in the pores of the coarser material, in deeper layers as well as deposited on top of the coarser material.

The field column experiments were carried out from June to September 2016. The Plexiglas columns were buried at six different locations (Fig. 4A) in streams within the sedimentation basin and were left there during one to eight weeks (SI Fig. 2). The columns, with an inner diameter of 9 cm and a height of 20 cm, were equipped with a bottom outlet consisting of a filter foil and an outlet port connected to a PVC tube (2 m) to ensure the outflow (Fig. 4B). The columns were filled to the height of 17 cm with the same rounded quartz sand used in the laboratory experiments. An armour layer of approximately 1 cm, consisting of gravel from the study area, was added on top. The columns were buried in the temporarily drained streambed at a depth where the top of the columns were slightly flooded. The sites were documented by GPS data and marked with a stick. In total eleven columns were recovered successfully after individual exposure periods that were co-determined by changing weather conditions. In addition, some columns were found above the water level since the streams changed the channels, but those were not considered for this study. All columns were checked subsequently to their recovery for intact water flow through. Afterwards, they were carefully transported by keeping them vertically in a backpack downhill and by train to the laboratory. The flow rate was measured accurately in the laboratory. Afterwards, the bed material was dissected into 1 cm layers. For each layer, the amount of particles smaller than 100 μm was determined by wet sieving, drying, and weighing.

3. Results

In this chapter, we present the results of six laboratory and three field experiments. The laboratory experiments were evaluated in

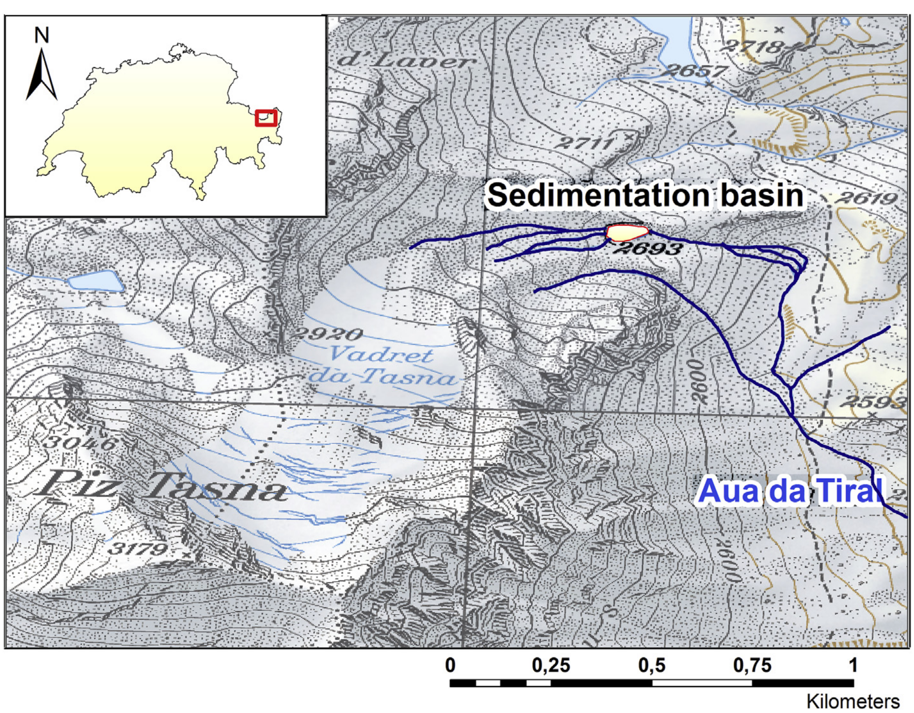

Fig. 3. Study area North East of Piz Tasna, Switzerland. The sedimentation basin, where the field experiments were carried out, is crossed by the Aua da Tiral stream. Map from www.swisstopo.admin.ch, locator map from services.arcgis.com.

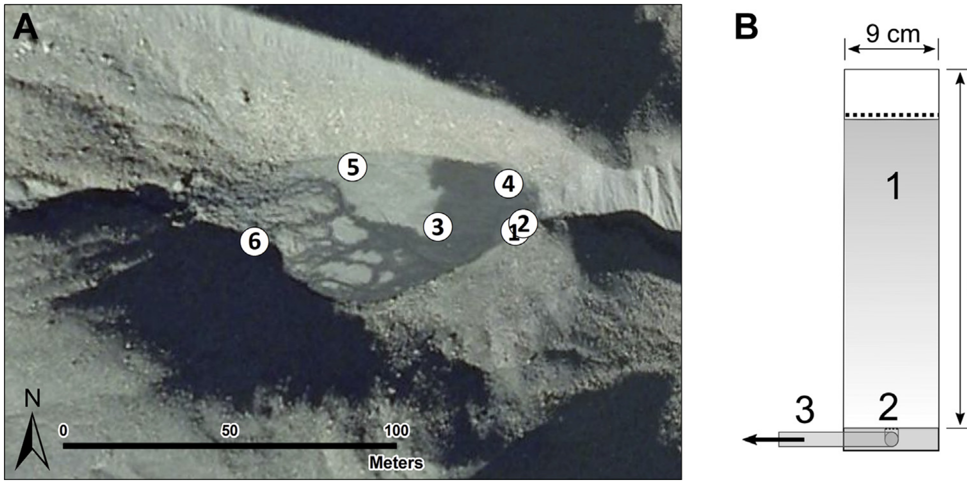

Fig. 4. Field column experimental design. (A) Sedimentation basin with column bury sites, where three columns where buried at Sites 1 and 3, two columns at Site 4 and one column at Sites 2, 5, and 6; (B) Plexiglas column filled with quartz sand (1) with a bottom outlet, closed by a filter foil (2), and connection port for a tube (3). Aerial photograph ©Google 2010.

pairs where only one parameter was varied while keeping all others constant. For the field column experiments, the only controlled parameter was the bed material while all others were governed by naturally varying hydrological conditions.

3.1. Laboratory results

All column experiments in the laboratory showed clogging with Z_C ranging from 1.5 to 18.0 cm (Table 1). A clearly visible sealing layer was observed for almost all experiments. The degree of clogging in terms of flow rate and pressure reduction varied strongly, as well as the clogging depth Z_C, and the transition pattern from clogged to non-clogged parts (images in Table 1). Table 1 gives an overview of the laboratory experiments with the specified parameters and the resultant clogging patterns. Arrows indicate the experimental pairs with the varied parameters ratio $d_M/(d_{SP}*\sigma)$, shape of bed material, initial flow rate, and electrolyte concentration.

Fig. 5A presents the pressure data for experiment *400r_SP1_v1 _Ca*. The graph shows the pressure reduction over the course of the experiment in 2 h steps. At the start of the experiment a linear pressure increase with depth is observed. Even though the increase reminds to a hydrostatic profile, pressure is not hydrostatic and the piezometric head decreases with depth. As the experiment progresses, pressure is reduced at all depths, but not uniformly with the strongest reduction located at around 2–3 cm depth, reached within the first 6 h. Afterwards, the process of pressure reduction is slowed substantially, approaching a steady state. Qualitatively, the pressure reduction exhibited similar patterns for the different experiments, while quantitatively they differed. For example, the pressure reduction for Experiment *400r_SP1_v1_Ca* was more pronounced with a maximum difference of 12.4 mbar, in contrast to 3.7 mbar for Experiment *400r_SP1_v1*. The total maximum pressure reduction ranged between 3 mbar for Experiment *400r_SP1_v1* and 14 mbar for Experiment *210a_SP1_v2*.

Fig. 5B shows the flow rate over time for each experiment. Two experiments, *400r_SP2_v2* and *210a_SP1_v2*, were carried out with an initial flow rate of about 2 mL/s, whereas the other four were started with approximately 1 mL/s. The flow curves exhibited different temporal patterns. *210a_SP1_v2* showed a distinct plateau before a more rapid decrease started after 1.5 h. This time point coincided with that at which the clogging depth was visually observed in photographs. Similar results were observed for the other experiments. All laboratory experiments showed a flow rate decrease of at least one third. In Experiment *210a_SP1_v1*, this point was reached after 45 min, after 2.5 h in Experiment *400r_SP2_v2* and after approximately 4 h in the remaining three experiments. The left Y axis shows the global hydraulic conductivity values that are in the order from 0 to 0.3 mm/s. The local K values for Experiment *400r_SP1_v1_Ca averaged* at the very beginning 7.1E-5 m/s. After 10.6 h, K has decreased to 1.0E-5 m/s in the non-clogged and to 1.4E-6 m/s in the clogged part. Consistent with our findings, Schälchli (1992) observed in his gravel bed experiments a substantial reduction of the hydraulic conductivity in the course of the experiment with K values decreasing from 5E-5 to 5E-6 m/s in the top layer.

3.2. Field results

The eleven field experiments resulted in a variety of clogging profiles, despite the single controlled parameter (bed material) not being varied. The apparent clogging depths Z_C ranged from 0.5 to 13 cm (images in Table 2 and SI Fig. 3a and b). In some cases, the armour layer was partly removed, leading to damage or removal of clogged layers. The results from the field represent a moment in time in the evolution and destruction of clogging layers. Brunke (1999) summarized three phases for the formation of clogged layers: the first phase is characterized by initial bridging of pores that does not affect the hydraulic conductivity, and the second phase by the retention of finer material and significant reduction of hydraulic conductivity. During the third phase the hydraulic conductivity reaches a steady minimum and in the bed pores particles are transported no longer. In the field a fourth phase, the damage of the clogged layer, is important and would lead again to the first phase. The condition of the recovered field columns depends on the evolution phase, and the phases can change rapidly due to uncontrolled and unsteady field conditions. Representative results were obtained from the eleven field columns, since they contained a variety of phases. We assume that the clogging depth does not change further, if a sealing layer has developed (no further particle penetration into the bed material) and as long as the armour layer stays intact.

The flow rates measured in the laboratory revealed that an intact armour layer can reduce flow rates by more than one order of magnitude. Columns with an intact versus disturbed armour layer

Table 1
Overview of results from the six laboratory experiments. Data includes suspended particles and bed material characteristics, modulation of parameters for each experiment, as well as photographs of each column at the end of the experiment with clogging depth Z_C.

Experiments	400r_SP1_v1	400r_SP2_v1	400r_SP2_v2	210a_SP1_v1	210a_SP1_v2	400r_SP1_v1_Ca
Independent variables						
SP diameter d_{SP}	Cat. 1 8.2 µm	Cat. 2 15.6 µm	Cat. 2 14.8 µm	Cat. 1 8.9 µm	Cat. 1 8.9 µm	Cat. 1 10.1 µm
Bed material diameter d_M	400 µm	400 µm	400 µm	210 µm	210 µm	400 µm
Ratio $d_M/(d_{SP}*\sigma)$ [1]	36.7	19.3	20.4	15.7	15.7	29.8 [2]
Bed material shape	round	round	round	angular	angular	round
Initial flow rate	1 [mL/s]	1 [mL/s]	2 [mL/s]	1 [mL/s]	2 [mL/s]	1 [mL/s]
Additional Ca^{2+}	no	no	no	no	no	yes
Photographs of column at the end of each experiment. Red line: filling height of quartz sand [cm] with armour layer on top. Red dotted line: approximate Z_C	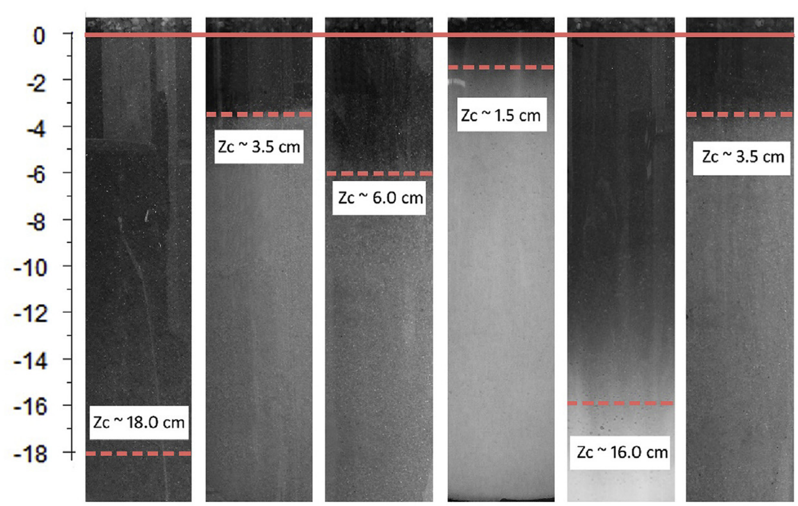					

The arrows, linking two experiments, present experimental pairs that differ in the marked parameter, all given diameters are d_{50} values
1 σ (standard deviation defined as $\sigma_M = SQRT(d_M^{85} / d_M^{15})$ d_M = 400: σ = 1.34, for d_M = 210: σ = 1.53
2 Calculated with d_{SP} before Ca^{2+} was added, aggregation not considered

exhibited flow rates from 15 µL/s to 21 µL/s and 330 µL/s to 1350 µL/s, respectively. Where the armour layer remained intact, the field results, indicated by Z_C and flow rate reduction, were comparable to laboratory findings. Nevertheless, the clogging and sealing layers in the field columns appeared to be more heterogeneous than those in the laboratory. In the field, the sealing layers and the sealing effect often were more pronounced than in the laboratory experiments (images in SI Fig. 3). Three of the eleven field column experiments were consecutively buried at Site 3. These three experiments with their final state of armour layer, minimal and maximum intrusion depths and resulting flow rates were representative for the entire body of field experiments. The dissection of the bed material of the field columns 3a, 3b, and 3c and the quantitative analysis of captured SP showed a profile decreasing exponentially with depth (profiles of captured SP in Table 2).

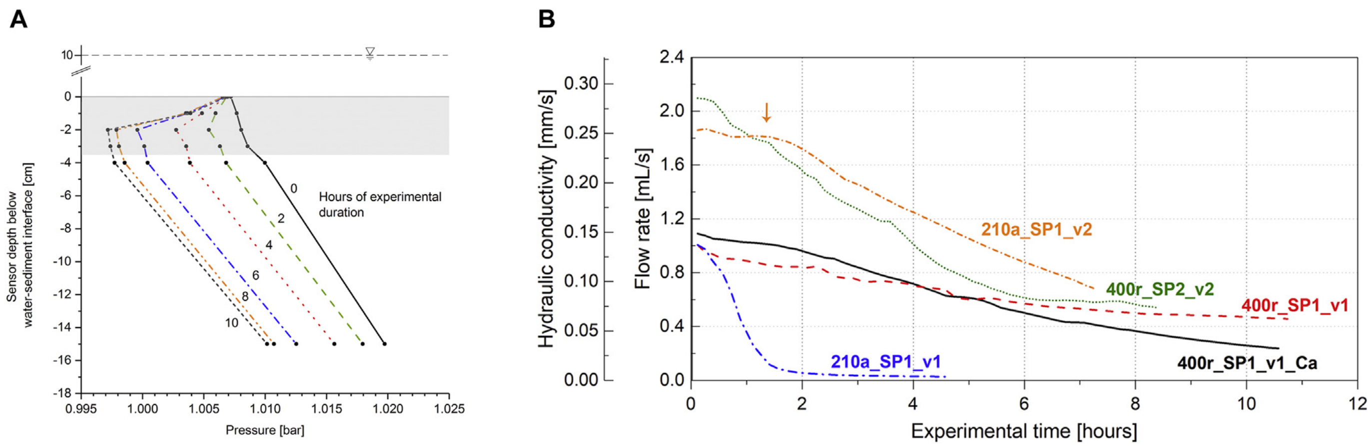

Fig. 5. Pressure und flow results from the laboratory experiments. (A) Pressure profiles for Experiment 400r_SP1_v1_Ca after 0, 2, 4, 6, 8, and 10 h. The changes in pressure were most pronounced around 2–3 cm depth in the first 6 h and slowed toward a steady state after 8 h. The light grey area indicates the final clogging depth of the column (B) Flow patterns with two experiments carried out with doubled initial flow rates (Q). Several experiments exhibited a rapid decrease after a certain period, e.g. 210a_SP1_v2 after 1.5 h. This time point also marks when the maximum clogging depth is reached (arrow). The left Y axis shows the hydraulic conductivity (K) that was calculated from the flow rate (Q) according to K=(Q/A)/(dh/dL), where dh is the hydraulic head [m] and dL is the length of the quartz bed [m]. The conversion is based on Experiment 400r_SP1_v1_Ca, where dh and dL were 0.19 m and 0.20 m, respectively.

4. Discussion

Hypothesis 1. The maximum bed-to-grain ratio where clogging occurs increases with the fineness of SP.

Fig. 6 shows the results of our six laboratory experiments and three field cases. On the same figure, we also plotted previous literature results obtained from flume experiments with sand-sized SP, reviewed by Huston and Fox (2014). Based on ten reviewed studies, the authors defined a critical bed-to-grain ratio $d_M/(d_{SP}{*}\sigma)$ of 27 for sand-sized SP as the maximum ratio where clogging still occurs. Note: for the description of the particle-size distribution, many studies used the geometric mean instead of d_{50} values. The difference can be significant in the case of non-Gaussian particle size distributions, which is true for our particles. In general, we used d_{50} values.

Our Experiment *400r_SP1_v1* with a bed-to-grain ratio $d_M/(d_{SP}{*}\sigma)$ of 37 still resulted in clogging. Although this is so far a singular result, a higher critical ratio for finer SP is reasonable when considering the following: In the case of fine SP, attractive surface forces gain importance (Benamar et al., 2007; Brunke, 1999; Schälchli, 1992; Valdes and Santamarina, 2006) due to an increase in the surface to weight ratio. At a certain size range, both chemical and physical interactions influence clogging. Benamar et al. (2007) suggest the transition of influence from physical to chemical variables at a size range of SP between 0.1 and 10 μm. At SP > 10 μm physical forces, such as hydrodynamics, gravity and inertial forces dominate. In contrast, Brunke (1999) suggested the dominance of physical forces for the particle range above 30 μm and the dominance of physicochemical interactions for particles down to 1 μm.

The laboratory experiments were designed in pairs to examine the influence of certain parameters. For the corresponding pairs *400r_SP2_v1* vs. *400r_SP2_v2* and *210a_SP1_v1* vs. *210a_SP1_v2*, the initial flow rate was varied by a factor of two. In both cases a doubling of the flow rate resulted in a considerable increase in the clogging depth Z_C. This observation is consistent with observations by Benamar et al. (2007) and Alem et al. (2015). They stated that higher pore flow velocities favour the transport of larger particles, leading to a deeper intrusion of SP. The hydraulic conductivity, as a measure of the ease with which water can move through pores, also reflects the clogging process. Experiment *400r_SP1_v1_Ca* showed a stronger hydraulic conductivity reduction in the clogged part in contrast to the non-clogged part. This agrees with the findings by Datry et al. (2015) who proposed the measurement of hydraulic conductivity in the field as an indicator for the degree of clogging.

The corresponding pair *400r_SP1_v1* vs. *400r_SP2_v1* showed that a higher ratio $d_M/(d_{SP}{*}\sigma)$ also led to a larger Z_C. In this case, the smaller the SP are in relation to the bed material, the further they intrude until they are eventually retained in the pores. As long as no parameter other than the bed-to-grain ratio was varied, we observed a linear relation between Z_C and bed-to-grain ratio. Concerning the shape of the bed material (*400r_SP2_v1* vs. *210a_SP1_v1*), Z_C is slightly larger for the round sand in comparison to the angular material. With respect to the different shapes, one should consider that our round material exhibits a wider size range than the angular material, resulting in smaller pores and thus a promotion of clogging. Hence, the influence of the shape is not clear in this case. In general, another aspect that can influence the clogging process is the interaction between bed material and suspended particles that is not only a function of size but also of surface properties. Rehg et al. (2005) showed in their clogging experiment that differently treated kaolinite particles resulted in different clogging patterns. SP with less interaction with bed materials remained more mobile.

Hypothesis 2. Higher Ca concentrations (in the order of mM) cause smaller clogging depths than at lower concentrations.

Experiment *400r_SP1_v1_Ca* was carried out as link between the low-electrolyte laboratory experiments and the field column experiments. The chosen Ca^{2+} concentration of 0.8 mM was relatively low but comparable to field conditions. Electrolytes influence the thickness of the diffuse double layer and hence, the tendency of SP to aggregate. This was confirmed in pre-experiments by the observation of enhanced coagulation and sedimentation after Ca^{2+} addition. In Experiment *400r_SP1_v1_Ca* the addition of Ca^{2+} led to a reduced clogging depth and a stronger pressure drop in the clogged layers, compared to Experiment *400r_SP1_v1*. However, for the correct interpretation of this experiment and the determination of the ratio $d_M/(d_{SP}{*}\sigma)$ a proper quantification of the SP enlargement would be needed.

The existence of a critical Ca^{2+} aggregation concentration for promotion of particle aggregation implies that waters with considerable electrolyte contents are not affected by a higher concentration of electrolytes. Nevertheless, the investigation of

Table 2
Overview of three field column experiment results. Data includes suspended particle and bed material characteristics, and the profile of captured suspended particles in gram captured particles per gram bed material.

Experiments	FC_3a	FC_3b	FC_3c
	28.06.16 - 20.07.16	20.07.16 - 16.08.16	16.08.2016 - 03.09.2016
Independent variables			
SP diameter range found in the field	8.2 to 20.8 μm, diameter mean values: 10.3 to 29.7 μm Size ranges from d_{10} = 2 μm to d_{90} = 62.2 μm		
Bed material	Diameter d_M (d_{50} value, quartz sand): 400 μm (σ^1 = 1.34)		
Ratio $d_M/(d_{SP}*\sigma)$	Range: 11.0 to 27.8		
Bed material shape	Shape of particles: round (ESEM images, SI Fig.2 a)		
Photographs of columns after recovery from field. Red dotted line: approximate Z_C. Depth profile: Amount of captured SP in column	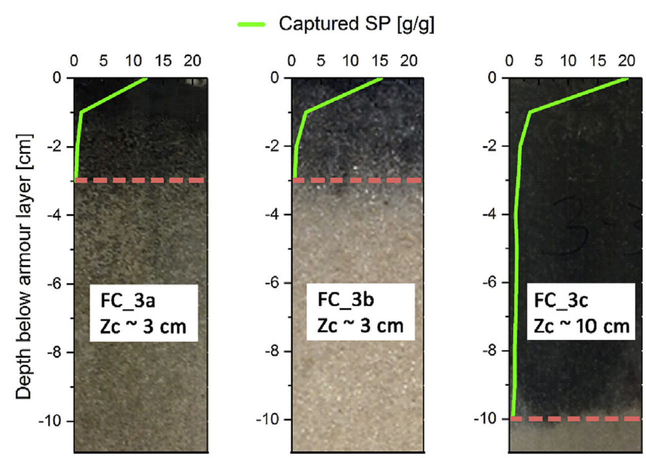		

1 σ: standard deviation defined as $\sigma_M = SQRT(d_M^{85} / d_M^{15})$, all used diameters are d_{50} values

higher electrolyte concentrations is relevant since local geogenic conditions and anthropogenic activities may cause those in low-electrolyte waters.

Overall, the results suggest that the aggregation of SP affects size and shape, and consequently the deposition morphology and the clogging degree.

Hypothesis 3. Field experiments generally exhibit a higher degree of clogging than laboratory experiments.

The field experiments can be best compared to the laboratory Experiment *400r_SP1_v1_Ca*, where the electrolyte concentration was elevated and hence, closest to field conditions. Field and laboratory results compared well regarding the clogging depths Z_C and the measured flow rates. In general, the columns in the field clogged faster than in the laboratory. Evidence for the faster clogging in the field was given by a lower amount of SP captured below the armour layer, in comparison to similar laboratory experiments. Lower amounts of SP captured below the armour layer in the field in comparison to laboratory experiments suggest that clogging might be promoted by field conditions. This is consistent with the finding of laboratory experiments by Siriwardene et al. (2007), who reported that clogging is accelerated by water level fluctuations and slowed down by elevated water levels. Most of our field columns exhibited a thick and more heterogeneous sealing layer with low water infiltration rates. This may be caused by a broader grain-size distribution of SP and bed material compared to laboratory conditions, as well as by an unsteady flow regime, since deposition depends on flow (Fries and Trowbridge, 2003). An increase in turbulence could jeopardize the comparability. In the field, an order-of-magnitude estimate of the friction velocity can be made as $u^* = SQRT(g\ R_h\ I_s) \sim 1$ cm/s, where g (9.81 m/s^2), R_h (0.1 m) and I_s (~0.0001) are the gravitational acceleration, the hydraulic radius and the bed slope, respectively. The velocity fluctuations decay exponentially in the permeable layer (Huston and Fox, 2016; Manes et al., 2009; Pokrajac and Manes, 2009). In our experimental design, the first attenuation occurs in the armour layer, where the intensity

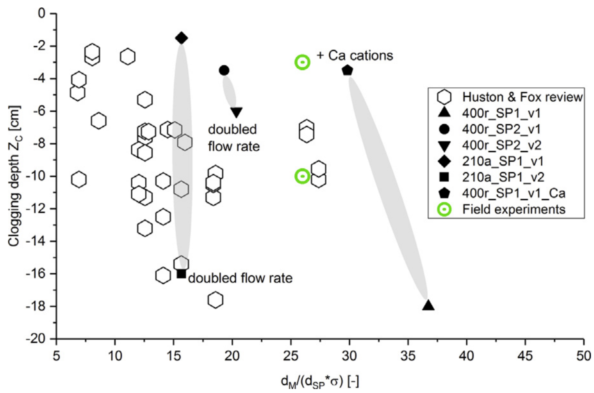

Fig. 6. Clogging depth Z_C to ratio $d_M/(d_{SP}{}^*\sigma)$ of this study's laboratory and field experiments in the context of other studies. Note, the shown field data points represent the three selected field experiments as shown in Table 2. All field experiments had the same bed material, and the identical mean SP diameter was used. Therefore, all field experiments exhibit the same bed-to-grain ratio. The hexagons represent experiments from four studies that worked with sand-sized suspended material and flume experiments from the review by Huston and Fox (2014). The grey connections indicate pairs of experiments, d_M and d_{SP} represent d_{50} values.

of velocity fluctuations is in the order of 1 mm/s. From there we expect a further sharp decrease to an intensity reaching the Darcy velocity within a few grain sizes in the quartz bed itself. This might influence the location of a sealing layer, but overall we do not expect a strong difference of the clogging depth and intensity. In the case of rough flow, however, grains might be displaced and the armour layer might be removed resulting in conditions that strongly differ from laboratory settings.

A broad gradation strongly favours clogging. Brunke (1999) emphasized the importance of larger SP (>30 μm) for an initial bridging of the pores. This affects the pore size distribution, but has no significant effect on hydraulic conductivity. Silt- and clay-sized SP are particularly important for the degree of clogging, since they significantly decrease the porosity and further consolidate the bed (Schälchli, 2002). From the previous investigations in the laboratory we can conclude for the field experiments that the stream flow velocity impacts the formation of the clogging layer, since it determines the concentration and size range of SP that are transported. Field measurements in fact showed that stream flow velocity and turbidity correlated strongly. Turbidity measurements revealed a strong variation in the particle concentration in the course of the experimental observations of 3 months. This is reflected by the heterogeneous clogging patterns (SI Fig. 3). Additionally, the discharge dynamics can affect the armour layer, and hence, can lead to the damage or removal of clogged layers. The three field column experiments 3a, 3b, and 3c demonstrated this relationship. Each of these columns was left buried at the same site for a period of two weeks, one after the other. Although they were filled with the same bed material, all of them exhibited different clogging depths and amounts of captured material (Table 2). During the experiments, the stream course and the discharge volume at this site varied, as observed from one field trip to the following.

In general, the degree of clogging is influenced by various parameters, such as Z_C, the reduction of porosity and hydraulic conductivity, and the strength of the sealing layer. The formation of a sealing layer especially affects most parameters. The slower a sealing layer forms, the more SP can infiltrate into the bed, leading to a deeper and stronger bed consolidation. A consolidated and thicker clogging layer is more difficult to remediate. Besides, a well-developed sealing layer results in lower pressure and a lower flow rate below. The formation of the sealing layer is probably most dependent on the concentration and particle-size distribution of SP.

The insights of clogging by silt-sized SP are crucial for the management of riverine systems. In comparison to coarse SP, clay- or silt-sized SP may clog pores faster and more pronounced, further contributing to negative ecological effects. The presence of silt-sized SP is often accompanied by poly-dispersivity that favours clogging. In addition, chemical interactions gain importance with silt-sized SP and also enhance clogging. Further the hydrological regime plays an important role. In prismatic channels, for instance, the hydrological variability is low, and hence the clogging process is slower compared to streams with high hydrological variability, allowing more particles to infiltrate and accumulate in the sediment before a sealing layer evolves. Additionally, the missing of wash-off effects of clogged layers in channels may lead to a permanently clogged riverbed.

5. Conclusions

For physical clogging, silt- and clay-sized SP play an important role. An original approach using vertical columns buried in the field and parallel laboratory experiments was presented. Various aspects were studied in the laboratory, such as the size of SP, the shape and size of the bed material, the influence of the electrolyte concentration, and the pore water flow velocity. Our results demonstrated that:

- The finer the SP, the higher the critical ratio $d_M/(d_{SP}{}^*\sigma)$. Our laboratory experiments complemented the existing studies on physical clogging by the results with silt-sized SP. Systems that contain clay- or silt-sized SP may be more exposed to faster clogging and a higher degree of clogging.
- The initial pore flow velocity and the ratio $d_M/(d_{SP}{}^*\sigma)$ have a strong influence on Z_C in the laboratory. We also showed that higher electrolyte concentrations lead to lower Z_C and a stronger pressure reduction in the clogging layer.
- The field and laboratory results compared well, in regards to the observed ranges of Z_C and measured flow rates. We found that the fluctuating hydrological regime in the field drives the clogging process. A broader grain size distribution and a fluctuating water level may lead to faster and more pronounced clogging, compared to laboratory results.

Funding

This research did not receive any specific grant from funding agencies in the public, commercial, or not-for-profit sectors.

Acknowledgements

Thanks to Ueli Schälchli for the input and discussion during the early stages of this work. James Fox and Davis Huston are gratefully acknowledged for giving additional helpful information on their paper. Further, we want to thank Annette Röthlisberger and Marion Rothaupt for the support in the laboratory. Daniel Braun, Toni Blunschi, Marius Floriancic, and Asel Maria Aguilar Sanchez are acknowledged for technical support, provision of devices, ideas, and information. We are grateful to the editor and the anonymous reviewers for their constructive comments that improved the manuscript.

Appendix A. Supplementary data

Supplementary data related to this article can be found at http://dx.doi.org/10.1016/j.watres.2017.09.015.

References

Adams, J.N., Beschta, R.L., 1980. Gravel bed composition in Oregon coastal streams. Can. J. Fish. Aquat. Sci. 37 (10), 1514–1521.

Alem, A., Ahfir, N.-D., Elkawafi, A., Wang, H., 2015. Hydraulic operating conditions and particle concentration effects on physical clogging of a porous medium. Transp. Porous Med. 106, 303–321. http://dx.doi.org/10.1007/s11242-014-0402-8.

Bai, B., Xu, T., Guo, Z., 2016. An experimental and theoretical study of the seepage migration of suspended particles with different sizes. Hydrogeol. J. 24, 2063–2078. http://dx.doi.org/10.1007/s10040-016-1450-7.

Benamar, A., Ahfir, N.-D., Wang, H., Alem, A., 2007. Particle transport in a saturated porous medium: pore structure effects. Compt. Rendus Geosci. 339, 674–681. http://dx.doi.org/10.1016/j.crte.2007.07.012.

Beschta, R.L., Jackson, W.L., 1979. The intrusion of fine sediments into a stable gravel bed. J. Fish. Res. Board Can. 204–210.

Bogen, J., Bonsnes, T.E., 2001. The impact of a hydroelectric power plant on the sediment load in downstream water bodies, Svartisen, northern Norway. Sci. Total Environ. 266, 273–280. http://dx.doi.org/10.1016/S0048-9697(01)00650-7.

Brunke, M., 1999. Colmation and depth filtration within streambeds: retention of particles in hyporheic interstices. Int. Rev. Hydrobiol. 84, 99–117. http://dx.doi.org/10.1002/iroh.199900014.

Cui, Y., Wilcox, A., 2008. Development and application of numerical models of sediment transport associated with dam removal. Sediment. Eng. Theory Meas. Model. Pract. ASCE Man. 110, 995–1020.

Datry, T., Lamouroux, N., Thivin, G., Descloux, S., Baudoin, J.M., 2015. Estimation of sediment hydraulic conductivity in river reaches and its potential use to evaluate streambed clogging. River Res. Appl. 31, 880–891. http://dx.doi.org/10.1002/rra.

Diplas, P., 1994. Modelling of fine and coarse sediment interaction over alternate bars. J. Hydrol. 159, 335–351. http://dx.doi.org/10.1016/0022-1694(94)90265-8.

Diplas, P., Parker, G., 1992. Deposition and removal of fines in gravel-bed streams. In: Billi, P., Hey, R.D., Thorne, C.R., Tacconi, P. (Eds.), Dynamics of Gravel-Bed Rivers. John Wiley & Sons Ltd, Chichester, pp. 313–329. http://dx.doi.org/10.1002/esp.3290180510.

Einstein, H.A., 1968. Deposition of suspended particles in a gravel bed. J. Hydraul. Div. 1197–1205.

Fox, J.F., 2016. Prediction of the clogging profile using the apparent porosity and momentum impulse. J. Hydraul. Eng. 142, 1–10. http://dx.doi.org/10.1061/(ASCE)HY.1943-7900.0001187.

Fries, J.S., Trowbridge, J.H., 2003. Flume observations of enhanced fine-particle deposition to permeable sediment beds. Limnol. Oceanogr. 48, 802–812.

Frostick, L.E., Lucas, P.M., Reid, I., 1984. The infiltration of fine matrices into coarse-grained alluvial sediments and its implications for stratigraphical interpretation. J. Geol. Soc. Lond. 141, 955–965. http://dx.doi.org/10.1144/gsjgs.141.6.0955.

Gibson, S., Abraham, D., Heath, R., Schoellhamer, D., 2010. Bridging process threshold for sediment infiltrating into a coarse substrate. J. Geotech. Geoenvironmental Eng. ASCE 136, 402–406. http://dx.doi.org/10.1061/(ASCE)GT.1943-5606.0000219.

Gibson, S., Abraham, D., Heath, R., Schoellhamer, D., 2009. Vertical gradational variability of fines deposited in a gravel framework. Sedimentology 56, 661–676. http://dx.doi.org/10.1111/j.1365-3091.2008.00991.x.

Grischek, T., Bartak, R., 2016. Riverbed clogging and sustainability of riverbank filtration. Water 8, 1–12. http://dx.doi.org/10.3390/w8120604.

Huston, D., Fox, J.F., 2016. Momentum-impulse model of fine sand clogging depth in gravel streambeds for turbulent open-channel flow. J. Hydraul. Eng. 142, 4015055 http://dx.doi.org/10.1061/(ASCE)HY.1943-7900.0001092.

Huston, D.L., Fox, J.F., 2014. Clogging of fine sediment within gravel substrates: dimensional analysis and macroanalysis of experiments in hydraulic flumes. J. Hydraul. Eng. 141, 1–14. http://dx.doi.org/10.1061/(ASCE)HY.1943-7900.0001015.

Jackson, W.L., 1981. Bed Material Routing and Streambed Composition in Alluvial Channels. Oregon State University, Forest Engineering (Hydrology).

Kennedy, M.J., Pevear, D.R., Hill, R.J., 2002. Mineral surface control of organic carbon in black shale. Science 295, 657–660. http://dx.doi.org/10.1126/science.1066611.

König, D., 2014. Particle-lacing in an Alpine Stream - Unpublished. Bachelor thesis. Swiss Federal Institute of Technology in Zurich (ETH), Department of Environmental Systems Science.

Manes, C., Pokrajac, D., McEwan, I., Nikora, V., 2009. Turbulence structure of open channel flows over permeable and impermeable beds: a comparative study. Phys. Fluids 21, 1–12. http://dx.doi.org/10.1063/1.3276292.

McDowell-Boyer, L.M., Hunt, J.R., Sitar, N., 1986. Particle transport through porous media. Water Res. 22, 1901–1921.

Nogaro, G., Datry, T., Mermillod-Blondin, F., Descloux, S., Montuelle, B., 2010. Influence of streambed sediment clogging on microbial processes in the hyporheic zone. Freshw. Biol. 55, 1288–1302. http://dx.doi.org/10.1111/j.1365-2427.2009.02352.x.

Pokrajac, D., Manes, C., 2009. Velocity measurements of a free-surface turbulent flow penetrating a porous medium composed of uniform-size spheres. Transp. Porous Media 78, 367–383. http://dx.doi.org/10.1007/s11242-009-9339-8.

Rehg, K.J., Packman, A.I., Ren, J., 2005. Effects of suspended sediment characteristics and bed sediment transport on streambed clogging. Hydrol. Process. 19, 413–427. http://dx.doi.org/10.1002/hyp.5540.

Rink-Pfeiffer, S., Ragusa, S., Sztajnbox, P., Vandevelde, T., 2000. Interrelationships between biological, chemical, and physical processes as an analog to clogging in aquifer storage and recovery (ASR) wells. Water Res. 34, 2110–2118.

Sakthivadivel, R., Einstein, H.A., 1970. Clogging of porous column of spheres by sediment. J. Hydraul. Div. 461–472.

Schälchli, U., 2002. Kolmation - Methoden zur Erkennung und Bewertung. Report by EAWAG (Swiss Federal Institute of Aquatic Science and Technology) and Schälchli, Abegg + Hunzinger - Flussbau AG Zürich.

Schälchli, U., 1992. The clogging of coarse gravel river beds by fine sediment. Hydrobiologia 235–236, 189–197. http://dx.doi.org/10.1007/BF00026211.

Siriwardene, N.R., Deletic, A., Fletcher, T.D., 2007. Clogging of stormwater gravel infiltration systems and filters: insights from a laboratory study. Water Res. 41, 1433–1440. http://dx.doi.org/10.1016/j.watres.2006.12.040.

Tourtelot, H.A., 1979. Black shale - its deposition and diagenesis. Clays Clay Min. 27, 313–321. http://dx.doi.org/10.1346/CCMN.1979.0270501.

Valdes, J., Santamarina, J., 2006. Particle clogging in radial flow: microscale mechanisms. SPE J. 11, 193–198. http://dx.doi.org/10.2118/88819-PA.

Vericat, D., Batalla, R.J., Garcia, C., 2006. Breakup and reestablishment of the armour layer in a large gravel-bed river below dams: the lower Ebro. Geomorphology 76, 122–136. http://dx.doi.org/10.1016/j.geomorph.2005.10.005.

Wooster, J.K., Dusterhoff, S.R., Cui, Y., Sklar, L.S., Dietrich, W.E., Malko, M., 2008. Sediment supply and relative size distribution effects on fine sediment infiltration into immobile gravels. Water Resour. Res. 44, 1–18. http://dx.doi.org/10.1029/2006WR005815.